# Multi-robot formations:
# One homography to rule them all

Gonzalo López-Nicolás, Miguel Aranda, and Carlos Sagüés

Instituto de Investigación en Ingeniería de Aragón. Universidad de Zaragoza, Spain.
gonlopez@unizar.es, marandac@unizar.es, csagues@unizar.es

**Abstract.** The problems of convergence to a desired configuration for a set of robots and leader-following in formation are considered in a framework where the robots have nonholonomic constraints, move in a plane and are observed by a calibrated flying camera, which provides the only sensory information used for the control. We propose a homography-based visual control method only requiring a priori single image of the desired configuration to perform the task. The proposed method consists of an image-based control scheme using the homography induced by the multi-robot system. Therefore, an interesting property is that the whole information regarding the multi-robot system is encapsulated in one single homography. The results show that the system is able to track the leader with the robots in formation despite the leader and camera motion are unknown.

## 1 Introduction

It is well known that some complex tasks cannot be adequately carried out by a single robot or its performance can be greatly improve by using multiple robots. From the variety of problems related with the topic of multi-robot systems, we focus in this paper in the goal of driving a set of robots to a desired configuration while following a leader, which is also part of the formation. A number of research works in this field focus on the problem of reaching and maintaining a robot team in a particular configuration [8] [13] [6].

Vision sensors have been extensively used for robot localization, navigation and control. Visual control is a wide field of research that has attracted the attention of many researchers [4]. In multi-robot systems, it is common to have a setup where each robot is equipped with a local perception system, and they share their information to accomplish the global task. This is the case, for example, of the localization method for multiple mobile robots presented in [5]. Another related work is [13], where groups of mobile robots are controlled to visually maintain formations, including the situation where communication between the robots is not available. The vision-based formation control with feedback-linearization proposed in [8] tackles the issue of switching between decentralized and centralized cooperative control.

Centralized multi-robot control approaches provide several advantages: they allow simple and cheap robots, and release their local resources by transferring expensive computations to an external computer. A centralized architecture is considered for the leader-follower control proposed in [6], where the perception system consists of a fixed

camera on the ceiling. In general, vision-based tasks become more robust when multiple view geometry constraints are imposed [11]. Particularly, the homography is a well-known geometric model across two views induced by a plane of the scene, and it has been used extensively in visual control [3], [7], [10].

In the framework considered here, the multiple robots are assumed to move in a planar surface and constrained to nonholonomic motion. The goal of the control scheme proposed is to drive the multiple robots to a desired configuration defined by an image previously taken of that configuration. One of the robots is designated as leader, and performs an arbitrary motion without following the commands of the control law used to maintain the formation. Therefore, the proposed control scheme allows the robots to track the leader in formation. The visual information is acquired by a flying camera looking downward that undergoes an arbitrary planar motion, in such a way that its translation is parallel to the robots motion plane and the rotation is parallel to the plane normal.

We propose a homography-based control approach that takes advantage of the planar motion constraint to parameterize the homography. The image features we employ to compute the homography are the projections of the multiple robots on the image plane. Then, the computed homography gives information about the configuration of the set of robots. In particular, from the homography we can determine if the configuration of the robots is rigid, i.e. they maintain the desired configuration defined by the target image, or nonrigid, meaning that the robots are in a different configuration. We propose an image-based control law where a desired homography is defined as a reference for the control in order to drive the robots to the desired configuration while tracking the leader robot. We can highlight several advantages of our approach. First, any arbitrary target configuration can be defined simply with one image, avoiding the need for information such as 3D measurements or relative positions between the robots. Another advantage is that in our method the camera can move, which allows it to carry out different or additional tasks independently of the control. Moreover, the control performance is not affected by the camera or leader motion, which can therefore be arbitrary.

This paper extends the work presented in [12] and [9]. The idea of homography-based control of a set of robots by using a flying camera was introduced in [12], where the camera performs an arbitrary motion that was constrained to be in a plane parallel to the floor. This constraint was avoided in [9], where the method was generalized and supported with real experiments. Additionally, we tackle the problem of collision avoidance when controlling multiple mobile robots [1], which has to deal with both inter-agent and external collisions. In that work, we use a potential-like collision avoidance method based on gyroscopic forces. We also proposed a purely image-based control strategy that drives the robots while minimizing the sum of the squared distances the robots have to travel [2]. That method features multiple cameras, each of them observing a subset of the robot team, and overcomes the field-of-view limitations of single-camera methods increasing their scalability by exploiting the advantages of both, centralized and distributed multi-robot control strategies. In this paper, we extend and test the proposal for a control law which carries out the multi-robot configuration and leader-following control task. The method is able to lead the robots to the desired configuration while

tracking one robot named as leader. The tracking task is hardened because the leader motion is not known a priori, but the control system handles it properly showing good performance.

The paper is organized as follows. Section 2 presents the parametrization of the homography and the definition of the desired homography for reaching the multi-robot goal configuration. The control law for the multi-robot system is presented in section 3. In Section 4 the performance of the proposal is illustrated in simulation. Finally, the conclusions of the paper are given in Section 5.

## 2 Homography-Based Scheme

The setup consists of a set of robots undergoing planar motion in the $x - y$ plane. The motion of the camera occurs in a plane parallel to the floor and the rotation of the camera is also parallel to the floor normal ($\mathbf{n}$). The motion of the camera is arbitrary and unknown while holding the previous constraints. One of the robots acts as leader, so that although it still belongs to the formation it also performs an arbitrary and unknown motion. In the following, we parameterize the homography in this framework and propose a procedure to define the desired homography that corresponds to the desired configuration of the multi-robot system.

Two perspective images can be geometrically linked through a plane by a homography $\mathbf{H} \in \mathbb{R}^{3 \times 3}$. This projective transformation $\mathbf{H}$ relates points of the plane projected in both images. Pairs of corresponding points $(\mathbf{p}, \mathbf{p}')$ are then related up to scale by $\mathbf{p}' = \mathbf{H} \mathbf{p}$. The calibrated homography can be related to camera motion and plane parameters as follows

$$\mathbf{H} = \mathbf{R} + \mathbf{T} \mathbf{n}^T / d \,, \tag{1}$$

where $\mathbf{R}$ and $\mathbf{T}$ are the relative rotation and translation of the camera, $\mathbf{n}$ is the unit normal of the plane with respect to the reference frame and $d$ is the distance along $\mathbf{n}$ between the plane and the reference position. In the framework considered, the position of the camera $(x, y, z)^T$ is constrained to the plane $x - y$ (i.e. $z = 0$) and rotation $\phi$ about the $z$-axis. This constraint yields

$$\mathbf{R} = \begin{bmatrix} \cos \phi & \sin \phi & 0 \\ -\sin \phi & \cos \phi & 0 \\ 0 & 0 & 1 \end{bmatrix} \,, \quad \mathbf{T} = \begin{pmatrix} t_x \\ t_y \\ t_z \end{pmatrix} \,, \tag{2}$$

with $\mathbf{T} = -\mathbf{R}(x, y, 0)^T$. In our framework, the mobile robots move in a planar surface that generates the homography. Besides, the camera undergoes planar motion: the translation is parallel to the plane and the rotation is parallel to the plane normal, i.e. the $z$-axis, and $\mathbf{n} = (0, 0, -1)^T$. Notice that the distance $d$ is the height of the camera with respect the motion plane of the robots. Therefore, the homography matrix is

$$\mathbf{H}_{rigid} = \begin{bmatrix} h_{11} & h_{12} & h_{13} \\ h_{21} & h_{22} & h_{23} \\ 0 & 0 & 1 \end{bmatrix} \sim \begin{bmatrix} \cos \phi & \sin \phi & -t_x/d \\ -\sin \phi & \cos \phi & -t_y/d \\ 0 & 0 & 1 \end{bmatrix} \,. \tag{3}$$

In our framework, the homography across two views can be computed from a minimal set of two point correspondences solving a linear system. In particular, the points

considered consist of the projection of the robots on the image plane, and each point correspondence gives two independent equations. Given that $\mathbf{H}_{rigid}$ is defined by seven unknown entries, and using the homography constraints $h_{11} = h_{22}$ and $h_{21} = -h_{12}$, a set of two point correspondences allows to determine the homography up to a scale factor by solving a linear system. Given that $h_{33}$ is never zero because of the particular form (3), the scale of the homography can always be normalized and fixed by this entry.

Similarly to the work [2], we wish to compute a 2D Euclidean transformation, but we will derive it from a homography parametrization simpler than (3). This requires a prior translation of the positions in the two sets of points. Here, this translation can be such that the points are expressed with respect to the respective global centroids. These centroids, $\mathbf{c}$ for the sets of points $\mathbf{p}$ of the current formation and $\mathbf{c}'$ for the sets of points of the desired formation $\mathbf{p}'$, are also expressed in the reference frame of robot and we assign

$$\mathbf{p}' := \mathbf{p}' - \mathbf{c}', \quad \mathbf{p} := \mathbf{p} - \mathbf{c} \tag{4}$$

The new coordinates transformed with the centroid are used hereafter (although in the following some comparison is provided with or without this transformation). Then, the two sets of transformed positions $\mathbf{p}'$ and $\mathbf{p}$ are used to compute a homography constrained to have the following form:

$$\mathbf{H}_{nonrigid} = \begin{bmatrix} h_{11} & h_{12} & 0 \\ h_{21} & h_{22} & 0 \\ 0 & 0 & h_{33} \end{bmatrix} \sim \begin{bmatrix} s\cos\phi & s\sin\phi & 0 \\ -s\sin\phi & s\cos\phi & 0 \\ 0 & & 0 & 1 \end{bmatrix}. \tag{5}$$
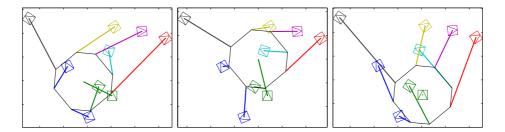
Unlike (3), the homography (5) is not Euclidean. However, as shown in [2], it can be computed linearly using SVD and allows to obtain the least-squares Euclidean homography that we are looking for, $\mathbf{H}^d$ as follows:

$$\mathbf{H}^d = \mathbf{H}_{nonrigid} \, diag(1/s, \, 1/s, \, 0) \,. \tag{6}$$

Each pair of robots induce a homography across two images, the current image and the image of the desired configuration. If all of these homographies are equal, the relative motion of the robots is rigid. Otherwise, if any of the homographies is different to the others, the relative motion of the set of robots is not rigid and they are not in the desired configuration. A desired homography computed using all robots needs to be defined in order to lead the robots to the desired configuration. The $\mathbf{H}_{nonrigid}$ relates each point $\mathbf{p}$ of the current image with the corresponding point $\mathbf{p}'$ in the desired formation image with $\mathbf{p}' = \mathbf{H}_{nonrigid} \, \mathbf{p}$. The desired homography $\mathbf{H}^d$ is used now to define the goal location of the robots (except the leader) in the image as

$$\mathbf{p}^d = (\mathbf{H}^d)^{-1} \, \mathbf{p}' + \mathbf{c} \,. \tag{7}$$

The effect of using or not the centroid (4) in the computation of the desired homography is shown in Fig. 3. In this example, nine robots are depicted in an arbitrary configuration. The desired configuration is an octagonal shape with the robots in the contour and the leader in the center. The target location of the octagon is drawn with thin line. Thick lines join each robot with its corresponding goal. The plots of the center

**Fig. 1.** Comparison of the desired image location for the robots provided by the goal homography in different cases for some instant time. The control law is performed without considering the centroid of the robot distribution (left), whereas it is considered in the next case (center). The last case translates the centroid of the desired robot locations to the leader (right).
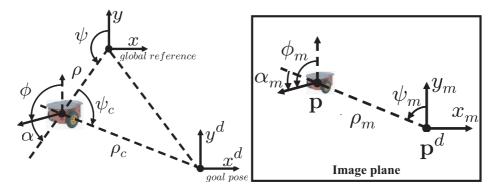
and left shows the difference of using or not the centroid in the point target location, respectively. This procedure minimizes the sum of squared distances between the current and desired positions of the robots to reach the desired configuration. It can be seen that considering the centroid the trajectories required to the robots are shorter. Furthermore, one of the robots acts as leader and will not follow the control scheme commands to reach the desired configuration. Thus, instead of using the centroid of the set of robots in (4), we propose to center the coordinates in the image coordinates of leader. In this way, the control law is not requiring any action from the leader to reach the formation. This is illustrated in the right plot of Fig. 3. This procedure improves the control performance as shown in the experimental section.

## 3  Visual Control Law

From the desired homography computed as explained in the previous section, we propose a control scheme to drive the robots to the desired configuration defined by an image of that configuration. Basically, in each iteration of the control loop, the flying camera takes a current image of the robots, the desired homography $\mathbf{H}^d$ is obtained and used in the control law to compute the robot velocities necessary to reach the desired configuration of the multi-robot system. These velocities are sent to the robots except the leader, which performs its arbitrary motion.

Different coordinate systems defined in the 3D space are depicted in Fig. 2 (left). The state of each robot is given by $(x, y, \phi)^T$, where $\phi$ is the orientation of the robot expressed as the angle between the robot body $y$-axis and the world $y$-axis. Each robot has two velocity inputs, the linear velocity $v$ and angular velocity $\omega$, with $v$ in the direction of the robot $y$-axis, and $\omega$ around the robot $z$-axis. The kinematics of each robot can be then expressed in general in polar or Cartesian coordinates as

$$\begin{cases} \dot{\rho} = v \cos \alpha \\ \dot{\alpha} = \omega - \frac{v}{\rho} \sin \alpha \\ \dot{\phi} = \omega \end{cases} , \quad \text{and} \quad \begin{cases} \dot{x} = -v \sin \phi \\ \dot{y} = v \cos \phi \\ \dot{\phi} = \omega \end{cases} , \tag{8}$$

**Fig. 2.** (Left) Coordinate systems from a top view of the 3D scene. The robot position is given by $(x, y, \phi)^T$ or $(\rho, \alpha, \phi)^T$ in the global reference. (Right) Coordinate systems on the image plane for each robot. Subindex $m$ denotes that the variable is defined on the image plane (the same variable without subindex $m$ refers to the 3D space). Point $\mathbf{p}$ is the image projection of a robot and $\mathbf{p}^d$ its location to reach the desired configuration of the multi-robot system.

respectively, being $x = -\rho \sin\psi$ and $y = \rho \cos\psi$. The alignment error $\alpha$ is defined as the angle between the robot body $y$-axis and the distance vector $\rho$ with $\alpha = \phi - \psi$.

We now introduce several variables, depicted in Fig. 2 (right), to define the state of each robot on the image plane with $(\rho_m, \psi_m, \phi_m)$. The origin of the coordinate system for each robot $\mathbf{p}$ on the image plane is placed in the desired location $\mathbf{p}^d$, i.e. the robots are in the desired configuration when all of them are in the origin of their respective references ($\mathbf{p}^d$). The alignment error on the image $\alpha_m$ is also defined as $\alpha_m = \phi_m - \psi_m$.
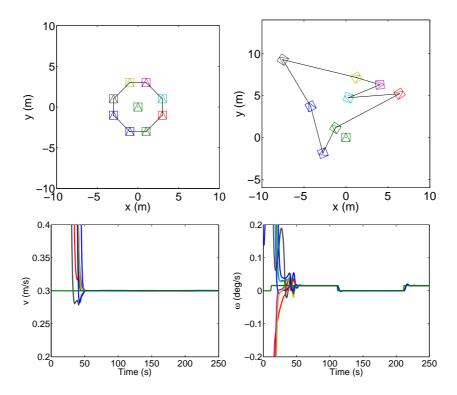
Finally, we define the control law in order to bring the robot team to the desired configuration as follows:

$$\begin{cases} v = -k_v \, \rho_m \\ \omega = -k_\omega \, (\alpha_m - \pi) \end{cases}, \tag{9}$$

where $k_v > 0$ and $k_\omega > 0$ are control gains. This control law drives the robots to their image target positions so that the team reaches the desired configuration while tracking the leader. The image projection of the distance to the desired position $\rho_m$ and the alignment error $\alpha_m$ are measured directly in the image plane.
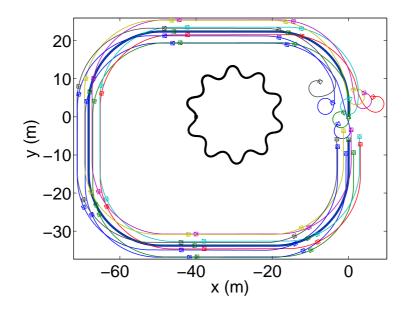
## 4 Simulation experiments

The approach presented in this work has been tested is simulation providing good results. In this section, we describe an example in order to illustrate the performance of the control scheme. The setup consists of a set of robots moving on the floor. In particular, nine robots are considered with one of them as the leader. The desired configuration is an octagonal shape with one of the robots, the leader, in the center. This is shown, together with the arbitrary initial configuration of the robots, in the first row of Fig. 3. The camera looking downwards is flying over the scene taking images of the set of

robots and, using the image of the desired configuration, the controller computes the desired homography that defines the goal location of the robots in the image plane. Note that the flying camera moves arbitrarily parallel to the floor plane and its motion is unknown for the control system. The velocity commands are sent to the robots, except the leader, to reach the desired formation. The leader does not accept commands and moves arbitrarily being its motion unknown for the control system.



**Fig. 3.** The desired configuration of the robots and their initial positions for the simulation presented are depicted, respectively, in the first row. The robots are distributed in the desired formation forming an octagonal shape with the leader robot in the centre. The linear and angular velocities given by the controller to follow the leader in formation are depicted in the second row.

The resultant velocities provided by the control law are shown in the second row of Fig. 3. The leader moves following a rectangular shape with rounded corners. The linear velocity of the leader is $v = 0.3$ m/s and the angular velocity is $\omega = \{0, 0.0157\}$ rad/s. It can be seen in the plots that the robots' velocities converge to the leader's velocities adequately in order to follow it. At the beginning, the velocities are higher as the initial configuration is very different to the desired one. Once the robots are in the formation, the control law tracks the leader velocities while keeping the robots in formation at the same time. A top view of the resultant motion of the set of robots and the flying camera is shown in Fig. 4. In this example, the flying camera follows a circular motion also
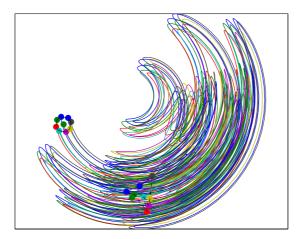
**Fig. 4.** Top view of the workspace showing the camera and robots motion in a simulation with the flying camera undergoing a circular motion compounded with sinusoids. The trajectory of the camera is depicted with a black line, starting at coordinates $(-40, 0)$. The initial positions of the robots are around $(0, 0)$ and the leader of the formation follows a rectangular shape motion anticlockwise. The path followed by the robots to reach the desired configuration and follow the leader is shown with coloured lines. The robots are depicted in some intermediate instants during the simulation.

compounded by sinusoids. The motion of the camera is depicted with black line and its initial location is $(-40, 0)\,m$ with height $50\,m$. The initial location of the robots is around the coordinates $(0, 0)$ and the path followed by the robots during the simulation is shown with coloured lines. The robots are also depicted in some intermediate instants to show that the correct formation is reached and maintained while tracking the leader.

The evolution of the robots in the image plane is depicted in Fig. 5. In this figure, the initial and final location of the robots is depicted with small coloured circles. Notice that the robots' trajectories in the image plane can be quite complex depending on the coupled motion between the robots and the arbitrary motion of the camera and the leader. Nevertheless, the proposed control law handles it correctly and in a simple way.
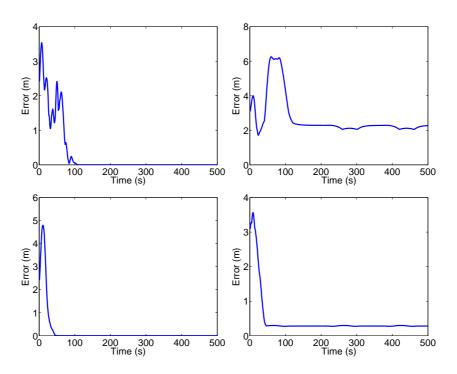
In order to evaluate the accuracy of the approach presented, we show in Fig. 6 the evolution of the error in the formation. The distance between each pair of robots in the the actual formation is measured and compared with the corresponding distances in the desired formation. The mean of the absolute difference values are then given as a measurement of the total error in the formation. Two different cases are considered in the error computation. In the first case, an additional simulation has been carried out where the control law is performed without considering the centroid of the set of robots in the computations (first row). In the second case, the centroid in considered and related with the leader robot of the formation (second row), this case corresponds with the simula-

**Fig. 5.** Trace of the robots in the image plane. The initial and last configuration of the robot formation is depicted with coloured circles. It can be seen that the traces of the robots in the image plane are quite complex because of the coupled motion between the robots and the arbitrary motion of the camera and the leader. Thanks to the homography-based approach, the control law handles correctly the problem independently of the complex trajectories in the image plane.

tion presented in this section. Additionally, the left plots in Fig. 6 corresponds to the error distances between robots without considering the leader, whereas the right plots consider the errors distances in where the leader is involved. It can be seen that the controlled robots reach the desired formation without error, independently of considering the centroid or not in the control law computations. The error distance in the formation regarding the leader is different to zero in any case and higher when not considering the centroid of the robots in the control law. Not considering the centroid means that the control law assumes that the leader cooperates in reaching the formation, but actually, the leader follows an arbitrary motion. Then, using the centroid centered in the leader, means that the control law realized that no cooperation comes from the leader and the robots compensate the leader motion to maintain the formation. Thus, reducing the formation error. Note that the motion of the leader is unknown and therefore, the control law cannot guarantee zero error while the leader is moving. The final error can be reduced by increasing the control law gains, but too high gains could reduce the system performance and lead to instability.

Finally, the evolution of the homography entries is depicted in Fig. 7. In particular, entries $h_{11}$, $h_{12}$, $h_{13}$, and $h_{23}$ are depicted given that $h_{22} = h_{11}$ and $h_{21} = -h_{12}$. Again, we separately present the homography entries of the set of robots without considering the leader (left column) and the entries of homographies where the leader is involved (right column). The robots reach the desired formation when the desired homography is finally reached. The results in terms of homography entries is coherent with the evolution of the error formation previously shown in Fig. 6. The homographies generated by the robots except the leader converge to the desired homography, i.e. they reach the desired formation, whereas the homographies that include the leader fluctuate
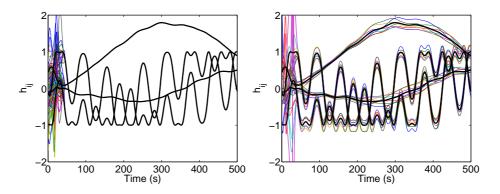
**Fig. 6.** Evolution of the error between the current formation and the desired formation. The distances between each robot in the current and desired formation are measured and the mean of the absolute error values is depicted. Different cases are tested: In the first row, we do not consider the centroid of the formation in the control law, contrary to the second row, where it is considered. In both cases, Left plot shows the error of all the robots in the formation without including the leader errors, whereas right plots show the errors of the leader with respect the rest of the robots in the formation.

around the desired homography with a small error, denoting that the robots follows the leader in formation with some tracking error. Notice that the final homography does not converge to a constant value given that it evolves because of the arbitrary motions of the camera and the leader of the formation.

## 5 Conclusion

The proposed control scheme is able to lead a group of robots to a desired configuration and follow the robot leader while maintaining the formation. The key point is that the control law is based on the computation of one single desired homography that allows to define the goal location of the robots in the image plane. The control scheme shows good performance, specially taking into account that neither the camera motion nor the leader trajectory are known or estimated. The final error distances in the formation during the navigation are zero between the robots but not with respect the leader, which presents some final error. This error regarding the tracking of the leader depends on its

**Fig. 7.** Evolution of matrix entries of the desired homography (thick lines) and actual homographies (thin lines) between the robots. Entries $h_{11}$, $h_{12}$, $h_{13}$, and $h_{23}$ are depicted. Left column shows the actual homographies except those where the leader robot is involved. Right column shows all the homographies in which the leader is involved. All the robots reach the desired homography with zero error except the leader, which is always moving away from the desired configuration.

dynamics and can be reduced by tuning the control gains. However, this error cannot be reduced to zero unless the leader stops or, as classical approaches consider, the motion of the leader is known a priori or estimated online.

## Acknowledgment

## References

1. Aranda, M., López-Nicolás, G., Mezouar, Y., Sagüés, C.: One homography to control multiple robots. In: Workshop on Visual Control of Mobile Robots (ViCoMoR) in conjunction with the IEEE/RSJ International Conference on Intelligent Robots and Systems. pp. 7–12 (2011)
2. Aranda, M., Mezouar, Y., López-Nicolás, G., Sagüés, C.: Partially distributed multirobot control with multiple cameras. In: American Control Conference. pp. 6323–6329 (2013)
3. Blanc, G., Mezouar, Y., Martinet, P.: Indoor navigation of a wheeled mobile robot along visual routes. In: IEEE International Conference on Robotics and Automation. pp. 3365–3370 (April 2005)
4. Chaumette, F., Hutchinson, S.: Visual servo control, part I: Basic approaches. IEEE Robotics and Automation Magazine 13(4), 82–90 (Dec 2006)
5. Chen, H., Sun, D., Yang, J.: Global localization of multirobot formations using ceiling vision SLAM strategy. Mechatronics 19(5), 617 – 628 (2009)

6. Chen, J., Sun, D., Yang, J., Chen, H.: Leader-Follower Formation Control of Multiple Non-holonomic Mobile Robots Incorporating a Receding-horizon Scheme. The International Journal of Robotics Research 29(6), 727–747 (2010)

7. Courbon, J., Mezouar, Y., Martinet, P.: Indoor navigation of a non-holonomic mobile robot using a visual memory. Autonomous Robots 25(3), 253–266 (2008)

8. Das, A.K., Fierro, R., Kumar, V., Ostrowski, J.P., Spletzer, J., Taylor, C.J.: A vision-based formation control framework. IEEE Transactions on Robotics and Automation 18, 813–825 (2002)

9. López-Nicolás, G., Aranda, M., Mezouar, Y., Sagüés, C.: Visual control for multirobot organized rendezvous. Systems, Man, and Cybernetics, Part B: Cybernetics, IEEE Transactions on 42(4), 1155 –1168 (Aug 2012)

10. López-Nicolás, G., Gans, N.R., Bhattacharya, S., Guerrero, J.J., Sagüés, C., Hutchinson, S.: Homography-based control scheme for mobile robots with nonholonomic and field-of-view constraints. IEEE Transactions on Systems, Man, and Cybernetics, Part B 40(4), 1115–1127 (2010)

11. López-Nicolás, G., Guerrero, J.J., Sagüés, C.: Visual control of vehicles using two-view geometry. Mechatronics 20(2), 315 – 325 (2010)

12. López-Nicolás, G., Mezouar, Y., Sagüés, C.: Homography-based multi-robot control with a flying camera. In: IEEE International Conference on Robotics and Automation. pp. 4492–4497 (2011)

13. Vidal, R., Shakernia, O., Sastry, S.: Following the flock: Distributed formation control with omnidirectional vision-based motion segmentation and visual servoing. Robotics and Automation Magazine 11(4), 14–20 (2004)